Archaeological investigations with TLS and GPR surveys and geomatics techniques

Vincenzo Barrile[1], Giuliana Bilotta[2] and Giuseppe M. Meduri[1]

[1] *University "Mediterranea" of Reggio Calabria, Department DICEAM, Reggio Calabria, Italy; vincenzo.barrile@unirc.it, giumed@libero.it*
[2] *University IUAV of Venice, Department of Planning, Ph.D. NT&ITA, Venice, Italy; giuliana.bilotta@gmail.com*

Abstract. This study is part of an interdisciplinary project aimed to define a religious path characterized by identification and definition of places of artistic, religious and cultural history. We conducted some archaeological surveys with the help of the GPR (Ground Penetrating Radar) techniques and TLS (Terrestrial Laser Scanner). Both these techniques are increasingly used, over the years, in the field of archaeological applications, with the ability to provide non-invasive, however, characterizing the objects or places of interest both spatially (with the TLS) providing information on the morphology of the ground, both in their internal structure, investigating in the material (with the GPR). However, with the GPR, to obtain highly accurate information from raw images (B-Scan) and easier to use and understanding in the field of archaeology, it is often necessary to improve their quality. Typically, this is possible with the aid of appropriate treatment of the raw image called focusing techniques. We tested various approaches of these techniques; starting from the raw data acquired through equipment georadar, were carried out numerical processing times of application of algorithms pre-processing of the image, for its improvement, and focusing developed. For the TLS were carried elaborations in post processing algorithms and tested best-fitting for the shape recognition. All the surveys are made with GPS measurements that carry out all the tracks. Laser scanner and GPR allow to make three-dimensional surveys of archaeological features and then everything is canalized in a WebGIS that allows the user to view the results.

Keywords. Archaeological survey, Radargrams, TLS,, WebGIS, Archaeological applications, Focusing treatment.

1. Introduction

Africo Vecchio is located in the heart of Aspromonte National Park at an altitude of about 700 m above sea level and founded in the ninth century AD. The community was abandoned after the great flood of year 1951 and moved along the Ionian coast, with the name of Africo. Near Africo Vecchio is the Byzantine church of S. Leo; behind it are supposed to be the ruins of an ancient monastery and / or ancient underground cisterns for collecting water. Investigations with laser scanners and ground penetrating radar are intended to reconstruct the morphology of the terrain recreating the three-dimensional model and to identify which areas could be subject to future archaeological digs.

The religious path object of discussion is located in the Aspromonte National Park (located in southern Calabria, Italy), situated in the southern part of the Apennine mountains (Figure 1) where, during the 5th to the 12th century AD , the Basilian monks also made a remarkable development of monasticism in southern Calabria. Many monasteries and churches were built by them at the time, and are representative of a cultural heritage of great historical and artistic value. The investigations carried out with GPR and TLS behind the church of S. Leo (Africo Vecchio, RC), were carried out, on the instructions of scholars, with the aim of identifying traces of a monastery and the possible presence of ancient water cisterns.

Figure 1. Geographical locations of Aspromonte National Park, the town of Africo Vecchio and of the churche of San Leo.

2. Methods

In the choice of materials, procedures and methods of study we took into account the need of using non-invasive techniques.

2.1. Survey with TLS

The acquisition of data in the portion of the soil investigated has been realized with the instrument Riegl LMS-Z420i with the execution of two positions instrumental and without the use of targets, not necessary for the type of processing performed. For the next recording operation of the scans, in fact, has been used the algorithm ICP (Interactive Closest Point) [1, 2], implemented in Matlab environment that allowed, without the aid of targets support, to generate a single point cloud representative of the investigated object.

The ICP algorithm iteratively applies a rigid roto-translation in space at one of the two clouds, considered to be mobile so that it overlaps in the best possible way to another cloud, regarded as fixed.

In an iteration, ICP assumes that the closest points correspond, calculates the absolute orientation and applies the rigid transformation obtained at Vj. In practice, in step 1 for each point of the mobile cloud (set Vi), are sought, within the cloud fixing points (closet point) contained within a sphere of a certain radius (multiple of a parameter introduced by the user) belonging to the set Vi and is kept as close will be taken the nearest of these, which will be considered to be the corresponding point. At step 2, with such matches found, the algorithm calculates the incremental transformation (Ri,j rotation matrix and translation vector T and solving the absolute orientation) applying the elements of Vj; when the Mean Squared Error is less a certain threshold, the iteration terminates otherwise returns to step 1.

The principle on which is based this algorithm is that the alignment between the two point clouds corresponds to the minimization of the Mean Squared Error of the instances minimum between the two objects, since the algorithm converges to a local minimum of the error [3]:

$$e = \sum_{i=1}^{N} \left\| x_i - \left(R_{yi} - T \right) \right\|^2 = min$$

$$C : V^j \,/\, \forall y \in V^j \exists x : min.distance(y,x) < \sigma$$

Figure 2. Point cloud after scan.

The three-dimensional model thus obtained was subsequently processed with an algorithm for texture mapping which allowed the "spread" on the cloud points of the photographic image thereby producing a realistic 3D model in Figure 3.

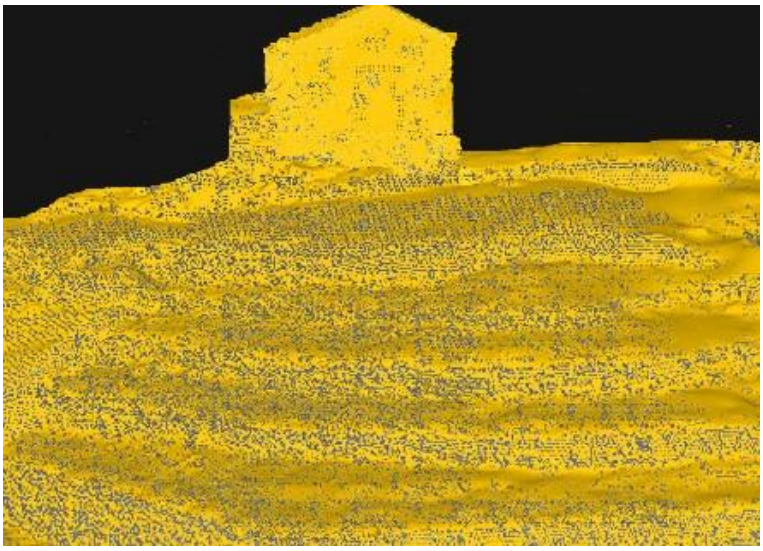

Figure 3. Result of the Texture Mapping.

The subsequent filtering step has as result in the first instance the removal of blunders and, subsequently, the identification of the points belonging to the land and the removal of those foreign to it (vegetation, buildings). At this stage, however, it was decided not to eliminate the points belonging to the church of S. Leo in order to use it, either as reference in modeling, both in the testing of the algorithms of best-fitting.

In this regard, we tested a best-fitting algorithm (by changing settings and parameters) which, by means of triangulation operations on the point cloud, converts points earned by the laser scanner in a surface representation through a function z = f (x , y) that, for a predetermined range of magnitude of the error and by virtue of information of proximity and adaptation, describes and approximates the curvature of the surface.

In particular, it has been used the local interpolation function z = ax2 + bxy + cy2 + dx + ey with five coefficients [4], determined with the method of least squares.

The phase of mesh finally models the type of geometry specified and transforms the raw 3D point set into a continuous surface.

2.2. Notes on Methods of Focusing within the GPR

In a section B-scan raw, obtained through a normal survey campaign with GPR monostatic, a buried object may appear in the form of hyperbolic track. With the term Wave Focusing (or migration) means a set of methods that can improve the quality of the B-scan, mitigating the effects which give rise to hyperbole, so that, in the results, the shape of the objects is processed and displayed more closer to their real physical size giving also a more accurate spatial location [5, 6 and references within]. Following a brief report on the techniques of focusing used for this article.

2.3. Diffraction Summation

When a GPR monostatic moves on a scan line along the y axis, a buried object located in the point of coordinates (y_α, z_α) gives rise to a hyperbolic track displayed in a B-scan, described by the following equation:

$$R_\alpha = \sqrt{z_\alpha^2 + (y_\alpha - y_\beta)^2} \qquad (1)$$

where R_α *i*s the distance between the measurement position $(y_\beta, z = 0)$ and the coordinates of the buried object scatterer (y_α, z_α). The technique Diffraction Summation is the simplest approach to the focusing of the trace representing the target [5, 6]. It operates as follows: if Ψ is the scalar field representative of the data collected along the scan line y, the scalar field focused Ψ_f can be obtained as the sum of each point inside the raw B-scan along the hyperbolic curve of diffraction defined by (1):

$$\Psi_f(y_\alpha, z_\alpha) = \sum_\beta \Psi\left(y_\beta, t = \frac{R_\alpha}{v_e}\right) \qquad (2)$$

where $v_e = v_f/2$ is the wave velocity in the middle obtained using model "exploding source" [6]. If the electromagnetic properties of the soil in which is buried the object slowly varying, can be used single speed v and for the whole extension in depth (ie, the medium can be considered homogenous) [6].

2.4. Kirchhoff migration

The method of Kirchhoff migration is based on the same principle characterizing the Diffraction Summation differing, however, for the treatment of "raw data" Ψ collected during scanning through the introduction of some correction factors. The scalar field focused Ψ_f can be described (in decent shape) as [5, 6 and references within]:

$$\Psi_f(y_\alpha, z_\alpha) = \frac{1}{2\pi v_e} \sum_\beta \Psi\left(y_\beta, \frac{R_\alpha}{v_e}\right) \frac{\cos(\theta)}{R_\alpha} \qquad (3)$$

where the term $cos(\theta)$, called "skew" [6], takes into account the fact that the normal to the wave front is not parallel to the normal of the scan line measurement and the term $1/R_\alpha$, named "spreading factor "[6], represents the losses of propagation of the waves in the ground.

2.5. F-K migration

FK migration (or migration of Stolt) can be considered as a variant of the phase shift method, valid only for a constant value of Fr. It can be shown that the expression of Ψ_f can be evaluated via inverse Fourier transform as:

$$\Psi_f(y,z) = \iint \tilde{\Psi}(k_y,\omega) e^{j(k_z(\omega)z + k_y y)} dk_y d\omega \qquad (4)$$

where k_y and k_z are the wave numbers, ω is the angular pulsation and $\tilde{\Psi}(k_y,\omega)$ is the Fourier transform of $\Psi(y, t)$. Taking into account that the wave number k_z is given by:

$$k_z = \sqrt{\left(\frac{\omega}{v_e}\right)^2 - k_y^2} \qquad (5)$$

Consequently, the (4) becomes:

$$\Psi_f(y,z) = v_e^2 \iint \frac{k_z}{\omega} \tilde{\Psi}(k_y,\omega) e^{j(k_z y + k_z z)} dk_y dk_z \qquad (6)$$

The relationship (6) is computationally significant: it allows to get the focusing data $\Psi_f(y, z)$ as simply the inverse Fourier transform of the product between k_z / ω and the two-dimensional Fourier transform of the raw data [5, 6 and references within].

2.6. SAR migration

The migration technique SAR can be derived considering a scenario in which are buried N scatterers, each with reflectivity ρ_α and coordinates (y_α, z_α) (per $\alpha \in \{1, ..., N\}$) [5, 6 and references within]. Consequently, $\Psi(y, t)$ can be modeled as:

$$\Psi_f(y,t) = \sum_{\alpha=1}^{\alpha=N} \rho_\alpha \exp\left(-j\frac{\omega}{v_e}\sqrt{z_\alpha^2 + (y_\alpha - y)^2}\right) \qquad (7)$$

If we consider the Fourier transform of (7) and the method of stationary phase is applied, it can be shown that the relationship (7) is expressible in the following way:

$$\tilde{\Psi}(k_y,k_z) = P(\omega) \sum_{\alpha=1}^{\alpha=N} \rho_\alpha \exp\left(-jz_\alpha k_z + jy_\alpha k_y\right) \qquad (8)$$

where $P(\omega)$ is the Fourier transform of the impulse GPR and k_z is given by the relation (5) [6]. If the GPR focused image $\Psi_f(y, z)$ is taken as:

$$\Psi_f = \sum_\alpha \rho_\alpha \delta(y - y_\alpha, z - z_\alpha) \qquad (9)$$

we get:

$$\Psi_f = \iint \frac{\tilde{\Psi}(k_y, \omega(k_z))}{P(\omega(k_z))} \exp(-jk_y y + jk_z z) dk_y dk_z \qquad (10)$$

An accurate assessment of (10) with an FFT (Fast Fourier Transform) requires equidistant points in the domain (k_y, k_z), which pose a problem [5, 6 and references within].

2.7. GPR survey

The investigations were carried out using the equipment GPR IDS RIS-K2 produced by Systems Engineering SpA, with an antenna 200 MHz. The profiles were acquired in continuous mode. The time window of acquisition was set to 250 ns and the sampling time of 0.5 ns. The GPR data were

stored during the survey campaign in the *.dt* format on a special notebook support. All survey operations were carried out in a day by a pair of operators. The data were processed off-line.

The processing sequence, subsequently listed, was adopted before making the treatment of focusing: *i)* the first time alignment, *ii)* dewow, *iii)* removal of the background, *iv)* time gain problem [5, 7 and references within]. All routine processing have been implemented in MatLab 2008b and executed on a PC support equipment 64-bit Intel Core 2 Duo 1.66 GHz 2 MB L2 cache and 4 GB ECC full-buffered DDR2 RAM.

Figure 4. GPR survey.

3. Results

The survey in the area adjacent to the church of San Leo (Figure 4) was carried out on an area of about 66 square meters with a rectangular grid. Were acquired 37 profiles 11.5 m in length, 0.31 m of equidistant, along the x direction, and profiles 18 of 5.5 m in length, equally spaced, 0.3 m along the y direction. The left side of Figure (5) shows the B-scan relative to a GPR profile (considered one of the most significant investigations of the campaign). One can observe a large and deep area that starts from the time of about 30 ns and descends to the bottom of the picture. At the time of about 10 ns, in this radargram, are identifiable (although not perfectly) different diffraction hyperbolas.

The speed of electromagnetic waves in the soil was assessed by analyzing the shape of this hyperbola yielding a value of 6.7 cm-1 nsec. In the right part of the Figure 5 and in Figure 6 are shown the images obtained using, respectively, the techniques of: Diffraction Summation, migration, Kirchhoff migration and FK. The result of the algorithm SAR algorithm has not been shown as very similar to that provided by the method FK.

From the results obtained, it is clear that the technique FK focuses on the traces representing the hyperbole in a slightly better than the other algorithms. In fact, the image does not show "ghost hyperbolas", which appear to occur in all other cases (an abnormality of this type could be interpreted as a cavity). In Table I shows the execution times of the methods exploited.

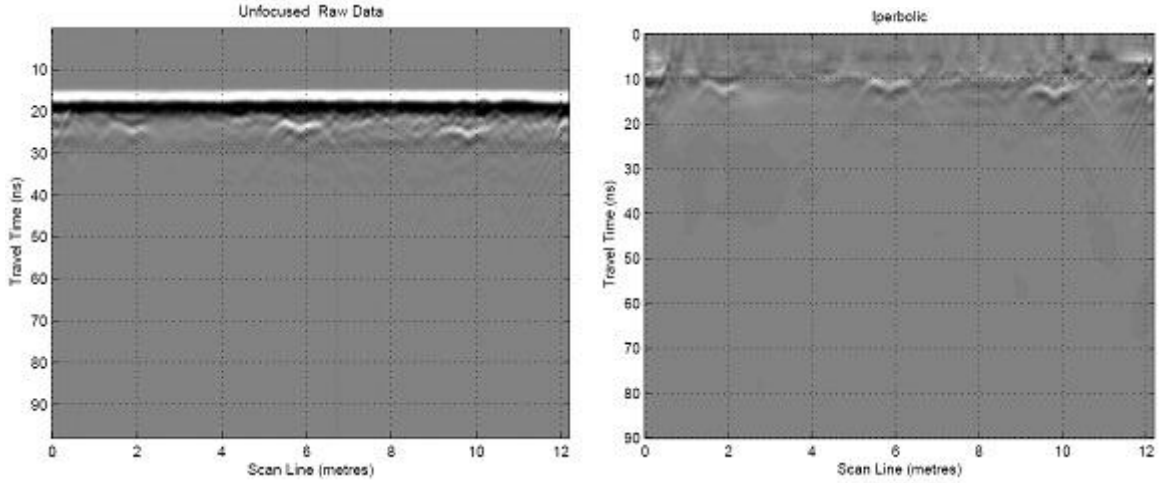

Figure 5. B-scan raw profile (GPR). and B-scan focused using the algorithm Diffraction Summation.

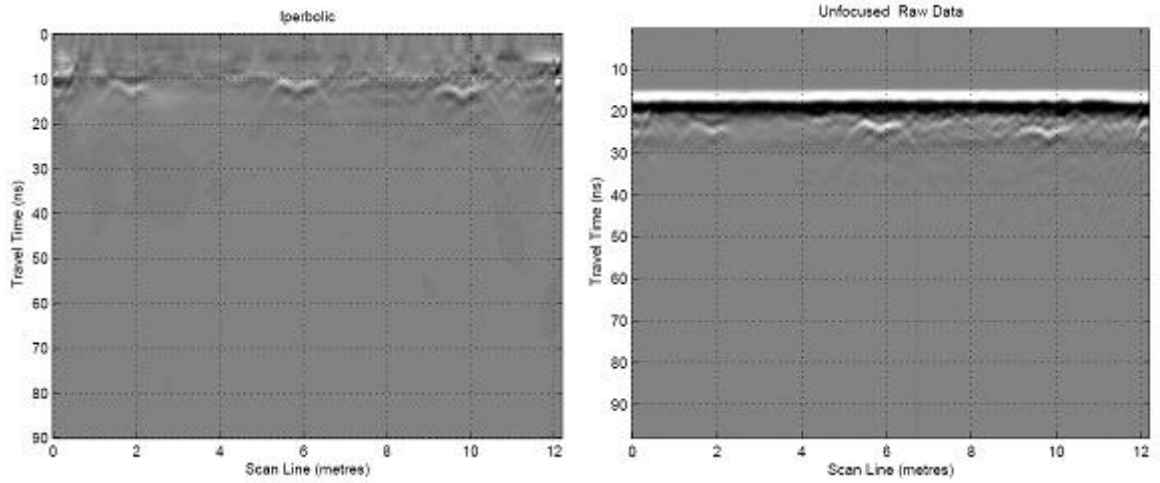

Figure 6. B-scan focused using the Kirchhoff algorithm and B-scan focused using the algorithm FK.

Table 1. Comparison of execution times of the algorithms used for focusing.

Method	GPR Profile
Hyperbolic Summation	13.28 sec
Kirchhoff Migration	89.87 sec
F-K migration	2.67 sec
SAR focusing	2.92 sec

4. Conclusions

In this work we reported preliminary results concerning the valuation of the various strategies to focus on the images collected in the GPR survey sites, located within the territory of the abandoned city of Africo Vecchio. Before the process of focusing the raw data, the latter were pretreated following a standard approach. The examples considered in this study seem to indicate the superiority of the algorithm FK compared to other techniques used.

As shown in Table 1, the algorithm FK is characterized by a lower computational burden compared to other methods applied, and this is an important feature for applications that work in real time. The overall findings made during the investigation seem to exclude the presence of subterra-

nean crypts, but indicate the presence of anomalies that require further investigation with a higher frequency antenna. These investigations will be carried out in a period subsequent to the preparation of this article.

References

[1] Chen, Y., Medioni, G., 1992. *Object modelling by registration of multiple range images*. Image and Vision Computing, 10: 145-155.
[2] Rusinkiewicz, S., Levoy, M., 2001. *Efficient variants of the ICP algorithm*. Third International Conference on 3D Digital Imaging and Modelling, Quebec City.
[3] Besl, P.J., McKay, N.D., 1992. *A Method for Registration of 3-D Shapes*. IEEE Transaction on pattern analysis and machine intelligence.
[4] Bhimji, S., 2005. *Curvature on Triangle Meshes*. School of Computing Science, Simon Fraser University.
[5] Daniels, J. D., 2004. *Ground Penetrating Radar 2th*, The Institution of Electrical Engineers, London.
[6] Turk, A. S, Hocaoglu K. A, Vertiy A. A., 2011. *Subsurface Sensing*. Wiley Series in Microwave and Optical Engineering, (Hoboken - NJ: Wiley-Blackwell) 890 pp..
[7] Masini, N., Persico, R., Rizzo, E., 2012. *Some Examples of GPR Prospecting for Monitoring of the Monumental Heritage*. Journal of Geophysics and Engineering, vol.7, 190–199.
[8] Orlando, L., 2007. *Georadar Data Collection, Anomaly Shape and Archaeological Interpretation - A Case Study from Central Italy*. Archaeological Prospection, vol.14, 213–335.
[9] D'Agostino, E., 2005. *Da Locri a Gerace. Storia di una diocesi della Calabria bizantina dalle origini al 1480* (Soveria Mannelli - CZ: Rubbettino Editore) 289 pp.
[10] Leucci, G., 2002. *Ground-penetrating Radar Survey to Map the Location of Buried Structures under Two Churches*. Archaeological Prospection, vol.9, 217–228.
[11] Barrile, V., Meduri, G.M., Angiulli, G., Decarlo, D., Isernia, T., 2012. *Caratterizzazioni ed indagini in ambito archeologico con GPR e TLS*. ASITA 2012.